



Insight into the rapid growth of graphene single crystals on liquid metal *via* chemical vapor deposition

Shuting Zheng¹, Mengqi Zeng^{1*}, Hui Cao¹, Tao Zhang¹, Xiaowen Gao¹, Yao Xiao² and Lei Fu^{1,2*}

ABSTRACT Previous reports about the growth of large graphene single crystals on polycrystalline metal substrates usually adopted the strategy of suppressing the nucleation by lowering the concentration of the feedstock, which greatly limited the rate of the nucleation and the sequent growth. The emerging liquid metal catalyst possesses the characteristic of quasi-atomically smooth surface with high diffusion rate. In principle, it should be a naturally ideal platform for the low-density nucleation and the fast growth of graphene. However, the rapid growth of large graphene single crystals on liquid metals has not received the due attention. In this paper, we firstly purposed the insight into the rapid growth of large graphene single crystals on liquid metals. We obtained the millimeter-size graphene single crystals on liquid Cu. The rich free-electrons in liquid Cu accelerate the nucleation, and the isotropic smooth surface greatly suppresses the nucleation. Moreover, the fast mass-transfer of carbon atoms due to the excellent fluidity of liquid Cu promotes the fast growth with a rate up to $79 \mu\text{m s}^{-1}$. We hope the research on the growth speed of graphene on liquid Cu can enrich the recognition of the growth behavior of two-dimensional (2D) materials on the liquid metal. We also believe that the liquid metal strategy for the rapid growth of graphene can be extended to various 2D materials and thus promote their future applications in the photonics and electronics.

Keywords: graphene, single crystal, rapid growth, liquid metal, chemical vapor deposition

INTRODUCTION

Due to the marvelous physical and chemical properties, graphene with one atom thickness can be widely used in photonics and electronics [1–4]. What should be noted is that the reliable application is based on the premise of synthesizing high-quality graphene with high efficiency [5]. The grain boundaries and defects that are inherent in

the polycrystalline film will have a strong influence on the mechanical properties and electronic and heat transport in graphene. Therefore, large graphene single crystals are highly demanded for the future applications. Chemical vapor deposition (CVD) approach is regarded as the most promising method to obtain high-quality large-size graphene single crystals [6–9].

Many studies focusing on the growth of graphene single crystal on metal substrates usually adopted the strategy of suppressing the nucleation density by lowering the concentration of the feedstock. However, according to the classical two-dimensional (2D) crystal nucleation and growth theory, when given the insufficient feedstock, although only a small amount of atom clusters can reach the critical size and initiate the nucleation, the rate of the nucleation and the sequent growth will be simultaneously limited significantly. Obviously, an ideal synthesis of graphene single crystal involving the rapid nucleation with low density and rapid growth is urgently to be established. The substrate design should be the sally port since it determines the adsorption, diffusion and assembly steps in the CVD process.

In the usual case studied on the polycrystalline solid Cu, the nucleation of crystal preferentially occurs at the sites with high surface energy, such as the grain boundaries, defect sites, facet steps and impurities because the free electrons at the metal surface can significantly saturate graphene edges [10], inevitably leading to the inhomogeneous nucleation density and limited crystal size [5,11]. Previous studies [12,13] on the growth of large graphene single crystals mainly focused on the improvement of surface morphology and the decrease of chemical reactivity of the substrate assisted with relatively low input of feedstock, such as surface monocrystallization and surface oxidation passivation, leading to a retarded growth rate. It is notable that by

¹ College of Chemistry and Molecular Sciences, Wuhan University, Wuhan 430072, China

² Institute for Advanced Studies (IAS), Wuhan University, Wuhan 430072, China

* Corresponding authors (emails: zengmq_lan@whu.edu.cn (Zeng M); leifu@whu.edu.cn (Fu L))

continuously supplying oxygen, the energy barrier of the decomposition of the carbon feedstock is enormously reduced and the growth rate of graphene reaches up to $60\text{ }\mu\text{m s}^{-1}$ [14,15]. However, the size of the as-obtained graphene single crystals is limited to several hundreds of micrometers. In addition, locally feeding carbon precursors at a desired position is beneficial to the single nucleation and fast growth of graphene [16]. While such a strategy requires complicated design and experimental setup and the growth rate is also not so satisfying. So far, how to achieve the low-density nucleation and fast growth for large-size graphene single crystal remains a great challenge.

The emerging liquid metal catalyst possesses the characteristic of quasi-atomically smooth surface with high diffusion rate, which can avoid the defects and grain boundaries that are inevitable for solid Cu [17–19]. In principle, it should be a naturally ideal platform for the low-density nucleation and the fast growth of graphene. A good balance between the nucleation density and the growth rate can be achieved. However, the rapid growth of large graphene single crystal on liquid Cu has not received due attention. Here, we firstly purposed the insight into the rapid growth of large graphene single crystal on liquid metal. We have obtained millimeter-size high-quality graphene single crystal on liquid Cu. The rich free electrons in liquid Cu accelerate the nucleation of graphene, and in the meantime the isotropic smooth surface greatly suppresses the nucleation density. Moreover, the fast mass-transfer of carbon atoms due to the excellent fluidity of liquid Cu promotes the fast growth with a rate up to $79\text{ }\mu\text{m s}^{-1}$. We hope that our work on the growth speed of graphene on liquid Cu system can further extend the roadmap of the growth behavior of 2D materials on the liquid metal. We also believe that the liquid metal strategy for the rapid growth of graphene can be extended to various 2D materials and thus promote their future applications.

EXPERIMENTAL SECTION

CVD growth of graphene single crystal on liquid Cu

The commercial Cu foils with a thickness of $100\text{ }\mu\text{m}$ (99.999%, Alfa Aesar) and W foils (99.95%, Alfa Aesar) with a thickness of $100\text{ }\mu\text{m}$ were used to form liquid Cu-W substrate. One piece of $1\times 1\text{ cm}^2$ Cu foil was directly put onto the $1\times 1\text{ cm}^2$ W foil, and then they were placed in the center of the furnace (Lindberg/Blue M, HTF55322C) with 800 sccm (standard cubic centimeters per minute) Ar to clean the growth system. Then the stacked Cu/W

foils were heated to $1,086\text{--}1,120^\circ\text{C}$ in the atmosphere of Ar and H_2 . When the temperature was up to the target temperature, the solid Cu foil was melted into a liquid state and spread on the W foil. During the growth process of graphene, CH_4 with different flow rates was introduced for different durations. After finishing the growth, the CH_4 was turned off, and the furnace was naturally cooled down to room temperature.

Transfer of graphene single crystal grown on liquid Cu

The graphene was transferred onto the $300\text{ nm SiO}_2/\text{Si}$ substrate by employing the ‘bubbling transfer’ method for Raman and electrical measurement [20]. The Cu-W substrate covered by graphene was spin-coated with polymethylmethacrylate (PMMA) at a speed of 3,000 rpm, and then was baked at 170°C for 10 min. Subsequently, in the electrochemical bubbling process, the Cu-W substrate acted as a cathode, and a platinum foil was used as the anode. NaOH solution (1 mol L^{-1}) served as the electrolyte. A constant current of 0.05 A supplied by a direct current power (DH1720A-5) was employed to release the PMMA/graphene film from the Cu-W substrate. After that, the PMMA/graphene film was transferred onto the SiO_2/Si substrate and then was dried naturally followed by the removal of PMMA in the hot acetone. When TEM characterization was conducted, the PMMA/graphene film was transferred onto the Cu grid and the subsequent steps were the same.

Electrical measurement

The ultraviolet lithography was employed to get the electrode pattern. Subsequently, 5 nm Ti and 45 nm Au electrodes were successively deposited by thermal evaporation. The data of current (I)–voltage (V) were collected in a probe station (Keithley 4200) at room temperature under air.

Characterization

Optical images were taken with an optical microscope (Olympus DX51). Raman spectra and maps were collected with a micro-Raman spectrometer (Renishaw in Via, 532 nm excitation wavelength). Scanning electron microscopy (SEM) images were taken by a ZEISS Merlin Compact SEM. Transmission electron microscopy (TEM) images, corresponding selected area electron diffraction (SAED) patterns and high-resolution atomic images were obtained by a high-resolution TEM (JEM-2100) with the operating voltage of 200 kV and aberration-corrected high-resolution TEM (Model AC-HRTEM, FEI Titan) with the operating voltage of 80 kV. Electron back-

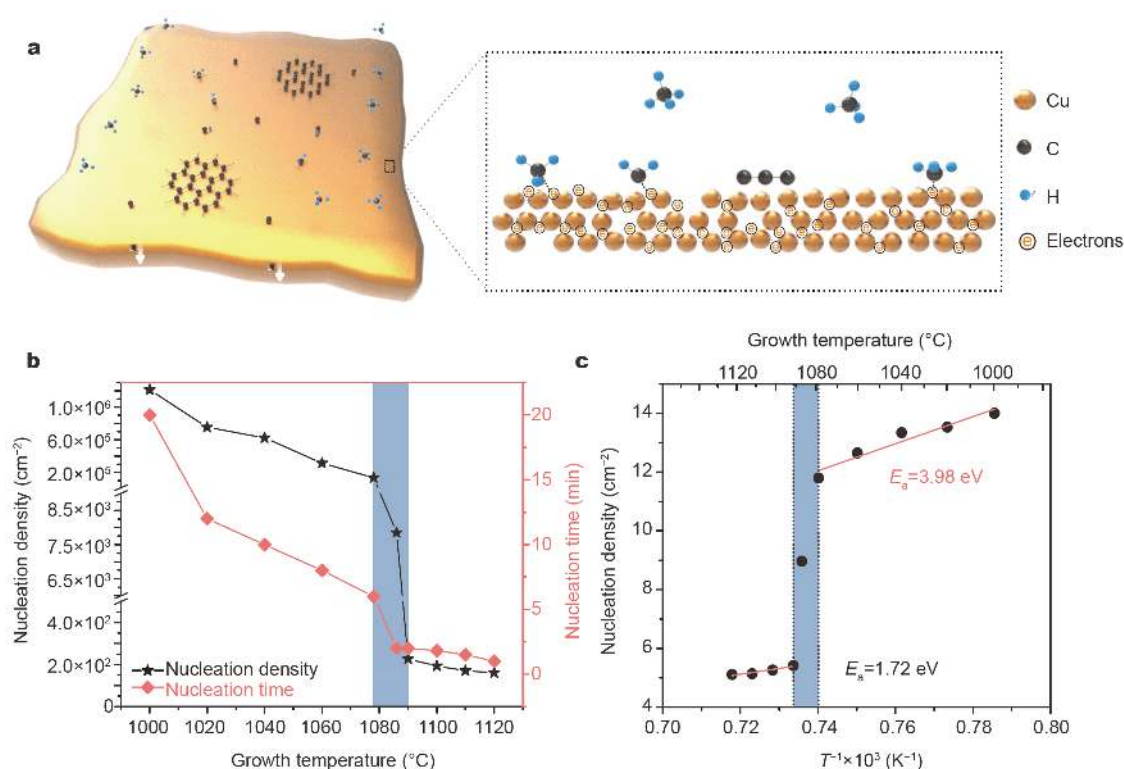


Figure 1 The nucleation of graphene on liquid Cu. (a) Schematic of the graphene nucleation on liquid Cu under CH₄ with extremely low concentration. The rich free electrons in liquid Cu can help grab the active carbon species for the graphene nucleation. (b) Plot of the nucleation density and nucleation time of graphene on Cu as a function of the temperature. (c) Arrhenius plot for the nucleation density of graphene on Cu.

scattered diffraction (EBSD) characterization was carried out by QUANTA FEG 450 at the operating voltage of 20 keV. The time of flight secondary ion mass spectra (TOF-SIMS) and maps were collected with ION-TOF (TOF SIMS 5). A Cs⁺ ion beam with the energy of 2 keV was employed to remove the layer while a Bi³⁺ ion beam with the energy of 30 keV was performed to analyze the material composition.

RESULTS AND DISCUSSION

Firstly, the nucleation of graphene on liquid Cu was investigated. CH₄ at an extremely low concentration (0.5 sccm/300 sccm/50 sccm CH₄/Ar/H₂) was introduced to critically trigger the nucleation. Fig. 1a illustrates the schematic diagram of the nucleation of graphene on liquid Cu surface. Fig. 1b shows the nucleation density and the nucleation time of graphene grains as a function of the growth temperature. Here, the nucleation time is defined as the duration time from the moment when CH₄ is introduced to the CVD furnace to the time when the graphene grains reach several microns. The typical SEM images corresponding to the graphene nucleation at the temperature ranging from 1,000 to 1,120°C are shown in

Fig. S1, from which the nucleation density can be statistically derived. The nucleation density of graphene is as high as 1.21×10^6 cm⁻² at the temperature of 1,000 °C on solid Cu with the nucleation time of 20 min, which is in the same order of magnitude with the previously reported studies [21–23]. With the temperature increasing from 1,000 to 1,060°C, the Cu keeps in a solid state and the nucleation density and nucleation time both decrease smoothly. However, when the heating temperature increases from 1,078 to 1,086°C, approaching the melting point of Cu (1,083°C), Cu begins to melt and the nucleation density of graphene exhibits a sharp decline with two orders of magnitude, and the nucleation time reduces from 6 to 2 min. As the temperature further increases, the nucleation density of graphene on liquid Cu starts to decline very slowly and finally reaches 2.26×10^2 cm⁻². It is obvious that both the nucleation density and nucleation time of the graphene grains exhibit a significant improvement along with the phase transition of the Cu. To evaluate the activation energy of the nucleation, Arrhenius function for the nucleation density of graphene on liquid Cu with temperature was conducted (Fig. 1c). For the nucleation on solid Cu, the

as-derived activation energy (E_a) is 3.98 eV, while for that on liquid Cu, the as-derived value is 1.72 eV. There indeed exists a significant difference of activation barrier between solid Cu and liquid Cu. The growth of graphene single crystals possesses a shorter nucleation time and a lower nucleation density on liquid Cu than on solid Cu.

To understand the difference between the graphene nucleation on solid Cu and liquid Cu, a deep insight into the elemental steps in the CVD process must be explored. Typical nucleation and growth stage of graphene are expected to experience the following elementary steps: (i) the adsorption of gas precursors; (ii) dehydrogenation of precursors on the catalyst substrates, leading to the formation of active carbon species; (iii) the diffusion of active carbon species; (iv) the formation of island with the critical size (critical nucleus), competing against the desorption; (v) the further growth of critical nucleus by incorporating C species to the graphene lattice [7–9].

With a low concentration carbon source, in the early stage of the nucleation, the carbon clusters were not stable and their energy tended to increase with the number of carbon atoms, leading to their decomposition. Only a small number of clusters can reach the critical size (n^*) with the Gibbs free energy increasing to the maximum value, which was the potential barrier in the nucleation of graphene. When the size of the clusters exceeded n^* , the Gibbs free energy started to decline with the enlargement of the clusters. The subsequent growth of the carbon clusters became faster than the nucleation. Therefore, the nucleation barrier determines the nucleation process, including the nucleation incubation time and the nucleation density.

The nucleation of graphene on solid Cu tends to occur at the active steps or defects rather than the terrace since the graphene edge can be saturated more effectively at these sites by the free electrons on the metal surface. Therefore, the nucleation density of graphene on solid Cu with a number of defects will be very high, leading to the graphene film with tremendous defects [24,25]. When the solid Cu surface is smoothened, the high nucleation potential barrier will hamper the high-efficiency nucleation. With the increase of the chemical potential of carbon (the concentration of the carbon precursor), the nucleation potential barrier will be totally overcome irrespective of the steps or terrace, leading to the nucleation with high density. It is nearly impossible to achieve the fast nucleation with low density.

However, the nucleation on liquid Cu with a fast speed and low density can be effectively achieved, attributed to the difference of electronic state and surface structure

between liquid Cu and solid Cu. On one hand, compared with the localization of d-electrons in the crystalline state, the delocalization of d-electrons occurs in a disordering state. There is a redistribution of the density of d-electrons among the neighbor atoms in liquid Cu [26–28]. Liquid metal is composed of positive ions which are scattered in the sea of electrons [29]. As shown in Fig. 1a, these rich free electrons on the liquid metal surface can significantly saturate the graphene edges and passivate the carbon clusters, and thus the formation energy of carbon clusters can be significantly lowered, which facilitates the fast nucleation [9,10]. The atom clusters would prefer to stably stick to liquid Cu surface rather than to re-vaporize during the deposition process. On the other hand, the surface of liquid Cu is isotropic and smooth, and the initial nucleation density will be quite low. In order to clarify the difference of the substrate surface structure between solid Cu and liquid Cu, EBSD was conducted on the solid Cu foil and the Cu foil after liquefaction and solidification, as seen in Fig. S2. Compared with the polycrystalline nature of solid Cu surface, the surface of solidified liquid Cu exhibits nearly uniform single crystal characteristic, which can act as a perfect platform to avoid defects and grain boundaries for low-density nucleation. In addition, when the size of the carbon clusters exceeds the critical nuclear size, the increment of Gibbs free energy will reduce with the increase of the carbon atoms. The graphene growth turns into a kinetic dominating process and the active carbon species prefers to attach to the edge of the already existing nuclei for graphene growth, rather than form new nuclei [30,31]. Thus, a rapid nucleation with a low nucleation density of graphene is achieved on liquid Cu.

Then, the growth of graphene on liquid Cu was systematically investigated. Fig. 2a–c present the SEM images of the individual graphene single crystals obtained at different growth time on liquid Cu at the temperature of 1,120°C. Here, the growth time of graphene is defined by the feeding time of CH_4 . At the growth time of 2 s, graphene grains with a size of $\sim 5\ \mu\text{m}$ can be clearly observed by SEM (Fig. 2a), confirming the rapid nucleation of graphene on liquid Cu surface again. The size of graphene quickly increases to $\sim 33\ \mu\text{m}$ at the growth time of 3 s (Fig. 2b), and further reaches to $\sim 112\ \mu\text{m}$ at the growth time of 4 s (Fig. 2c). The maximum growth speed is as high as $79\ \mu\text{m s}^{-1}$, which is faster than those reported in the previous work in Fig. 2e and Table S1 [12–14,16,30,32–35]. To the best of our knowledge, this is the first exploration of such exceptionally fast growth of graphene single crystal on

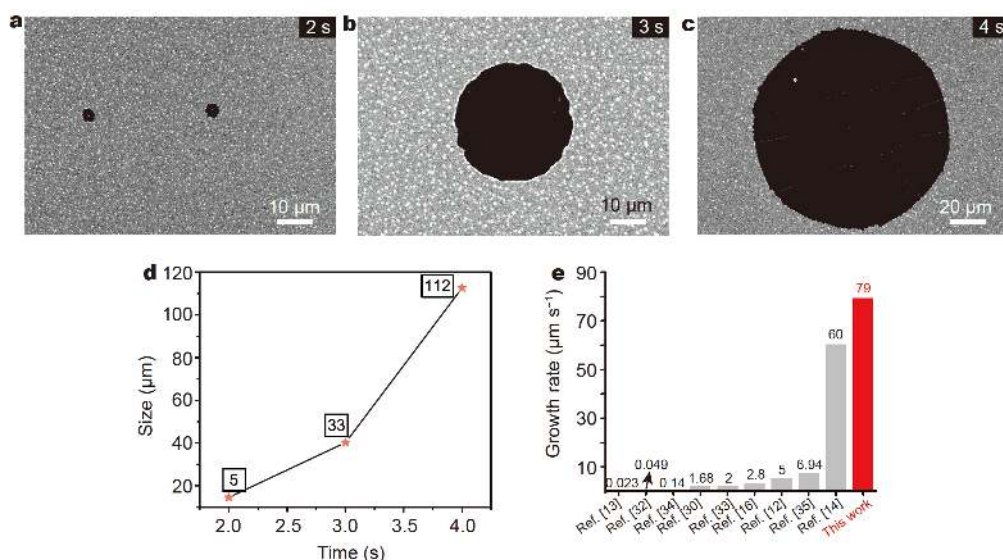


Figure 2 Time evolution of graphene single crystal grown on liquid Cu. (a–c) SEM images of graphene single crystals synthesized at $t=2$, 3 and 4 s. $t=0$ s is defined as the moment when CH_4 is introduced to the CVD furnace. (d) Plot of graphene size as a function of growth time. (e) Comparison of the growth rate of graphene in the recent literatures. The growth was conducted in the atmosphere of Ar/ H_2 / CH_4 (800 sccm/5 sccm/5 sccm) at $1,120^\circ\text{C}$.

liquid Cu surface, which encourages us to study the kinetics of fast growth of graphene single crystal. By contrast, the growth of graphene single crystal on solid Cu was also analyzed, as seen in Fig. S3. It can be seen that the nucleation time of graphene on solid Cu is much slower than that on liquid Cu. The growth rate of graphene on liquid Cu is almost two orders larger than that on solid Cu. The rapid growth of graphene single crystal on liquid Cu can be ascribed to the following aspects.

First of all, the nucleation density of graphene on liquid Cu is greatly reduced [36], favorable for the fast growth since the dissociative decomposed carbon atoms on the fluidic liquid Cu surface tend to attach to the as-formed graphene islands instead of forming new nuclei. Secondly, the evaporation of Cu atoms is much more pronounced for liquid Cu than that for solid Cu [37]. The collision between the copper vapor originating from liquid Cu and CH_4 gas is greatly enhanced, promoting the decomposition of CH_4 and producing highly active carbon species. Subsequently, the as-decomposed carbon atoms are prone to incorporate into the existing graphene islands. Thirdly, the migration potential barrier of precursors on liquid Cu is far lower than that on solid substrates. Liquid Cu exhibits a short-range order but a long-range disorder in the atomic configuration and is composed of abundant copper atoms, clusters and vacancies, which can facilitate the embedding of hetero-atoms [38]. Due to the

instability of the surface atoms in the clusters, it may transfer from the primary clusters to another, resulting in very weak binding force among the atomic clusters [28]. The intense thermal motion leads to a fluctuation of the interatomic distance and a dynamic change of the distribution of the vacancies, which facilitates the migration of the carbon atoms and increases their diffusion rate. The diffusion mass transport of carbon atoms on the liquid surface plays a significant role in the rate-determining step of graphene growth on liquid Cu. As shown in Fig. S4, when the growth temperature was increased, the surface tension of liquid Cu decreased and the as-related rate of diffusion of carbon species increased, leading to a higher growth rate and the formation of the larger graphene single crystals. To exclude the effect of the increase of the decomposed carbon concentration with the temperature, we conducted the growth of graphene at a higher flow rate of CH_4 . As seen in Fig. S5, the growth rate of graphene changes little and the size of the obtained graphene single crystals is nearly the same because the mass-transport *via* diffusion determined by the temperature is the rate-determining step for the graphene growth. In addition, to elucidate the mechanism and kinetics of the graphene growth on liquid Cu, carbon isotope labeling experiments were conducted with Raman spectroscopy. Specific Raman G bands at $1,525$ and $1,595\ \text{cm}^{-1}$ correspond to the signals of ^{13}C and ^{12}C graphene, respectively [39]. In

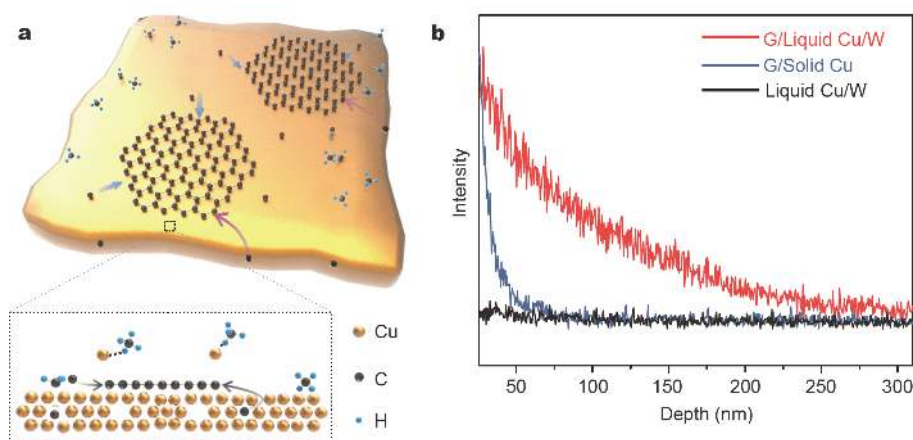


Figure 3 Fast growth mechanism of graphene on liquid Cu. (a) Schematic illustration of the precursor supply for the graphene growth on liquid Cu, which can both come from the surface adsorption and the bulk segregation. (b) TOF-SIMS characterizations to show the intensity profile of carbon along the surface of G/liquid Cu and G/solid Cu after graphene growth for 10 min, and liquid Cu after annealing for 10 min, respectively.

the growth of graphene on liquid Cu, $^{13}\text{CH}_4$ and $^{12}\text{CH}_4$ were sequentially introduced to the reaction zone, and the system was purged with 800 sccm Ar and 50 sccm H_2 for 2 min to reduce intermixing of the two isotopes. The statistical data show that the peak position of the G band of the as-obtained graphene is narrowly located at $1,562\text{ cm}^{-1}$ (Fig. S6a), indicating the uniform distribution of ^{13}C and ^{12}C , which is different from the situation for the graphene on the solid Cu [39]. Unlike the surface adsorption growth mode on solid Cu, the precursor supply for the graphene growth on liquid Cu can both come from the surface adsorption and the bulk segregation. Due to the rich vacancies in liquid Cu [38], carbon atoms can firstly diffuse into the metal bulk before segregating and precipitating toward the Cu surface just as the growth of graphene on Ni with high carbon solubility [39]. As a result, a uniform distribution of ^{12}C and ^{13}C atoms is expected to be obtained by sequential dosing of $^{12}\text{CH}_4$ and $^{13}\text{CH}_4$, and the as-produced graphene single crystals are composed of uniformly distributed ^{12}C and ^{13}C atoms, exhibiting the highly mixed G Raman band. Therefore, the precursor supply for the graphene growth on liquid Cu can be attributed to both the surface diffusion and bulk segregation (Fig. 3a). TOF-SIMS was carried out to exhibit the carbon distribution on the surface and sub-surface of the sample with high-accuracy depth profiling. In this study, depth-profiling SIMS measurements performed on graphene/liquid Cu/W (G/liquid Cu), graphene/Cu (G/solid Cu) and Cu/W (liquid Cu) elaborated the distinctly different carbon dissolution behaviors in the liquid and solid Cu (Fig. 3b). In the case of G/liquid Cu, an enrichment of

carbon was detected on the surface of liquid Cu after the substrate was exposed to CH_4 for a few minutes. The intensity of carbon content decreases slowly from the surface to the depth of 310 nm. However, a rapid monotonic decrease of carbon content occurs in G/solid Cu at the same depth analysis, which reveals a rather low saturation state of carbon content in solid Cu. By comparison, the carbon concentration along the profile in the pure liquid Cu remains the same, which can eliminate the background signal. In addition, carbon atoms sufficiently diffuse into the bulk of liquid Cu with the intensity map of SIMS shown in Fig. S7a, and there are nearly no carbon atoms diffusing into the bulk of the solid Cu as shown in Fig. S7b. The results confirm the different bulk segregation behaviors between liquid Cu and solid Cu. The binary contributions of the precursor supply, i.e., the surface adsorption and the bulk segregation, accelerate the growth of graphene.

Due to the low nucleation density, fast nucleation time and rapid growth rate, we achieved the rapid growth of large graphene single crystals on liquid Cu. As seen in Fig. 4a, graphene single crystals with the diameter of $\sim 2.6\text{ mm}$ can be seen directly from the naked eye. Fig. 4b exhibits the optical microscopy (OM) image of an as-transferred graphene crystal on a $300\text{ nm SiO}_2/\text{Si}$ substrate. The characteristic 2D and G bands are displayed with the intensity ratio (I_{2D}/I_G) larger than 2, exhibiting a monolayer feature. No discernible defect-related D band located at $\sim 1,350\text{ cm}^{-1}$ can be identified, demonstrating the high quality of the as-grown graphene (Fig. S8f) [40,41]. To confirm the single crystal characteristic of the graphene grains, Raman mapping

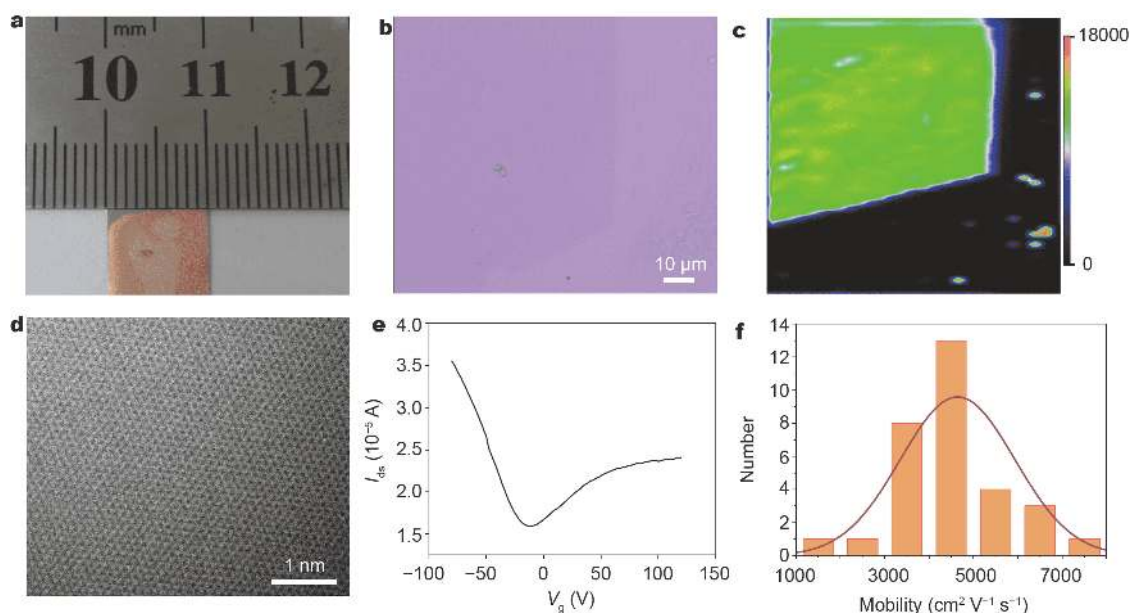


Figure 4 Large graphene single crystals grown on liquid Cu and the related quality characterizations. (a) Photograph of graphene single crystals grown on liquid Cu. (b) OM image of a corner of graphene single crystal transferred onto 300 nm SiO₂/Si substrate. (c) Intensity mapping of 2D band, corresponding to the region in (b), showing the uniformity of the graphene single crystal at macroscopic scale. (d) HRTEM image of graphene, revealing the perfect hexagonal honeycomb structure. (e) The typical transfer characteristic curve of the as-fabricated FET device based on the graphene single crystal grown on liquid Cu at room temperature. (f) A histogram plot of the mobility value distribution extracted from 30 devices.

(Fig. 4c) shows the 2D intensity mapping of a corner of a graphene crystal with a very uniform contrast, further indicating the high crystallinity of the as-grown large graphene crystal at the macroscopic scale. The microstructure of the graphene single crystal was evaluated by TEM. Single-layer characteristic is determined by counting the dark lines of the backfolded edge (Fig. S8b). The SAED patterns derived from different regions on an individual crystal show the same orientation, demonstrating its single crystalline characteristic (Fig. S8c–e). The single-layer feature and the superior crystallinity of the graphene crystal were further probed by the low-voltage, aberration-corrected, high-resolution TEM (Fig. 4d), which clearly revealed the perfect atom-scale six-fold symmetric single-crystal nature of the graphene without any detectable defect and vacancy. The electrical quality of the as-obtained graphene single crystal was evaluated through constructing back-gated field-effect transistors (FET) on 300 nm SiO₂/Si substrates. As shown in Fig. 4e, a typical transfer curve of the drain current (I_{ds}) as a function of the gate voltage (V_g) was collected under the ambient condition in the air. In addition, a histogram distribution of the derived carrier mobility value extracted from 30 FET devices is presented in Fig. 4f. The mobility is ranging

from 1,000 to 8,000 cm² V⁻¹ s⁻¹, reasonably confirming the high quality of the graphene single crystals grown on liquid Cu.

CONCLUSION

In summary, we have achieved the rapid growth of millimeter-size graphene single crystals on liquid Cu, taking advantage of the characteristic of liquid metal. The fast nucleation can be attributed to the rich free-electrons in liquid Cu, significantly lowering the nucleation energy barrier. And the low nucleation density is due to the low-defect and highly homogeneous isotropic liquid surface. The growth rate of the graphene single crystal on liquid Cu is up to 79 μm s⁻¹. And the fast growth is highly dependent on the low nucleation density, high diffusion rate and unique segregation mass-transfer mechanism in liquid Cu growth system. We believe the exciting results provide a new direction to the fast growth of large 2D material single crystals on the liquid metals.

Received 29 January 2019; accepted 16 February 2019;
published online 15 March 2019

- 1 Novoselov KS, Geim AK, Morozov SV, *et al.* Two-dimensional gas of massless Dirac fermions in graphene. *Nature*, 2005, 438: 197–200

- 2 Novoselov KS, Fal'ko VI, Colombo L, *et al.* A roadmap for graphene. *Nature*, 2012, 490: 192–200
- 3 Zeng M, Xiao Y, Liu J, *et al.* Exploring two-dimensional materials toward the next-generation circuits: from monomer design to assembly control. *Chem Rev*, 2018, 118: 6236–6296
- 4 Li K, Zhang J. Recent advances in flexible supercapacitors based on carbon nanotubes and graphene. *Sci China Mater*, 2017, 61: 210–232
- 5 Lin L, Deng B, Sun J, *et al.* Bridging the gap between reality and ideal in chemical vapor deposition growth of graphene. *Chem Rev*, 2018, 118: 9281–9343
- 6 Vlassioux I, Smirnov S, Regmi M, *et al.* Graphene nucleation density on copper: fundamental role of background pressure. *J Phys Chem C*, 2013, 117: 18919–18926
- 7 Safron NS, Kim M, Gopalan P, *et al.* Barrier-guided growth of micro- and nano-structured graphene. *Adv Mater*, 2012, 24: 1041–1045
- 8 Kim HK, Mattevi C, Calvo MR, *et al.* Activation energy paths for graphene nucleation and growth on Cu. *ACS Nano*, 2012, 6: 3614–3623
- 9 Wang L, Gao J, Ding F. Application of crystal growth theory in graphene CVD nucleation and growth. *Acta Chim Sin*, 2014, 72: 345–358
- 10 Gao J, Yip J, Zhao J, *et al.* Graphene nucleation on transition metal surface: structure transformation and role of the metal step edge. *J Am Chem Soc*, 2011, 133: 5009–5015
- 11 Geng D, Wang H, Yu G. Graphene single crystals: size and morphology engineering. *Adv Mater*, 2015, 27: 2821–2837
- 12 Wang H, Xu X, Li J, *et al.* Surface monocrystallization of copper foil for fast growth of large single-crystal graphene under free molecular flow. *Adv Mater*, 2016, 28: 8968–8974
- 13 Hao Y, Bharathi MS, Wang L, *et al.* The role of surface oxygen in the growth of large single-crystal graphene on copper. *Science*, 2013, 342: 720–723
- 14 Xu X, Zhang Z, Qiu L, *et al.* Ultrafast growth of single-crystal graphene assisted by a continuous oxygen supply. *Nat Nanotech*, 2016, 11: 930–935
- 15 Xu X, Zhang Z, Dong J, *et al.* Ultrafast epitaxial growth of metre-sized single-crystal graphene on industrial Cu foil. *Sci Bull*, 2017, 62: 1074–1080
- 16 Wu T, Zhang X, Yuan Q, *et al.* Fast growth of inch-sized single-crystalline graphene from a controlled single nucleus on Cu–Ni alloys. *Nat Mater*, 2015, 15: 43–47
- 17 Zeng M, Wang L, Liu J, *et al.* Self-assembly of graphene single crystals with uniform size and orientation: the first 2D super-ordered structure. *J Am Chem Soc*, 2016, 138: 7812–7815
- 18 Liu J, Fu L. Controllable growth of graphene on liquid surfaces. *Adv Mater*, 2018, 8: 1800690
- 19 Zeng M, Fu L. Controllable fabrication of graphene and related two-dimensional materials on liquid metals *via* chemical vapor deposition. *Acc Chem Res*, 2018, 51: 2839–2847
- 20 Gao L, Ren W, Xu H, *et al.* Repeated growth and bubbling transfer of graphene with millimetre-size single-crystal grains using platinum. *Nat Commun*, 2012, 3: 699
- 21 Hedayat SM, Karimi-Sabet J, Shariaty-Niassar M. Evolution effects of the copper surface morphology on the nucleation density and growth of graphene domains at different growth pressures. *Appl Surf Sci*, 2017, 399: 542–550
- 22 Liu L, Zhou H, Cheng R, *et al.* A systematic study of atmospheric pressure chemical vapor deposition growth of large-area monolayer graphene. *J Mater Chem*, 2012, 22: 1498–1503
- 23 Zhou H, Yu WJ, Liu L, *et al.* Chemical vapour deposition growth of large single crystals of monolayer and bilayer graphene. *Nat Commun*, 2013, 4: 2096
- 24 Lin L, Li J, Ren H, *et al.* Surface engineering of copper foils for growing centimeter-sized single-crystalline graphene. *ACS Nano*, 2016, 10: 2922–2929
- 25 Wood JD, Schmucker SW, Lyons AS, *et al.* Effects of polycrystalline Cu substrate on graphene growth by chemical vapor deposition. *Nano Lett*, 2011, 11: 4547–4554
- 26 Ross M, Boehler R, Errandonea D. Melting of transition metals at high pressure and the influence of liquid frustration: the late metals Cu, Ni, and Fe. *Phys Rev B*, 2007, 76: 184117
- 27 Shabanova IN, Kholzakov AV, Kraposhin VS. XPS study of transition metal electronic structure in crystalline and liquid states. *J Electron Spectr Related Phenomena*, 1998, 88–91: 453–455
- 28 Shabanova IN, Mitrokhin YS. The study of the atomic and electronic structures of liquid copper. *J Electron Spectr Related Phenomena*, 2004, 137–140: 569–571
- 29 Laidler KJ, Meiser JH. Physical Chemistry. Boston: Houghton Mifflin, 1999
- 30 Lin L, Sun L, Zhang J, *et al.* Rapid growth of large single-crystalline graphene *via* second passivation and multistage carbon supply. *Adv Mater*, 2016, 28: 4671–4677
- 31 Sun L, Lin L, Zhang J, *et al.* Visualizing fast growth of large single-crystalline graphene by tunable isotopic carbon source. *Nano Res*, 2017, 10: 355–363
- 32 Chen CC, Kuo CJ, Liao CD, *et al.* Growth of large-area graphene single crystals in confined reaction space with diffusion-driven chemical vapor deposition. *Chem Mater*, 2015, 27: 6249–6258
- 33 Babenko V, Murdock AT, Koós AA, *et al.* Rapid epitaxy-free graphene synthesis on silicidated polycrystalline platinum. *Nat Commun*, 2015, 6: 7536
- 34 Guo W, Jing F, Xiao J, *et al.* Oxidative-etching-assisted synthesis of centimeter-sized single-crystalline graphene. *Adv Mater*, 2016, 28: 3152–3158
- 35 Vlassioux IV, Stehle Y, Pudasaini PR, *et al.* Evolutionary selection growth of two-dimensional materials on polycrystalline substrates. *Nat Mater*, 2018, 17: 318–322
- 36 Geng D, Wu B, Guo Y, *et al.* Uniform hexagonal graphene flakes and films grown on liquid copper surface. *Proc Natl Acad Sci USA*, 2012, 109: 7992–7996
- 37 Guo W, Xu C, Xu K, *et al.* Rapid chemical vapor deposition of graphene on liquid copper. *Synth Met*, 2016, 216: 93–97
- 38 Zeng M, Tan L, Wang J, *et al.* Liquid metal: an innovative solution to uniform graphene films. *Chem Mater*, 2014, 26: 3637–3643
- 39 Li X, Cai W, Colombo L, *et al.* Evolution of graphene growth on Ni and Cu by carbon isotope labeling. *Nano Lett*, 2009, 9: 4268–4272
- 40 Zeng M, Tan L, Wang L, *et al.* Isotropic growth of graphene toward smoothing stitching. *ACS Nano*, 2016, 10: 7189–7196
- 41 Ferrari AC, Meyer JC, Scardaci V, *et al.* Raman spectrum of graphene and graphene layers. *Phys Rev Lett*, 2006, 97: 187401

Acknowledgements The research was supported by the National Natural Science Foundation of China (21673161) and the Sino-German Center for Research Promotion (1400).

Author contributions Fu L and Zeng M developed the concept and conceived the experiments. Zheng S, Zeng M, Cao H, Zhang T, Gao X and Xiao Y carried out the experiments. Zheng S and Zeng M wrote the

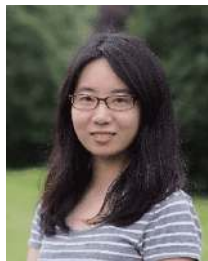
manuscript. Fu L revised the manuscript. All of the authors contributed to the data analysis and scientific discussion.

Conflict of interest The authors declare no competing financial interest.

Supplementary information The supporting information is available in the online version of the paper. (The nucleation density of graphene on Cu at different temperatures, EBSD characterizations conducted on solidified liquid Cu and solid Cu, comparison of the growth rate of graphene single crystal between our work and the reported literatures, the growth rate of graphene single crystal grown on solid Cu, effect of diffusion rate on the growth rate of graphene single crystal on liquid Cu, the identification of the effect of the diffusion rate on the growth rate of graphene single crystal on liquid Cu, carbon isotope labeling experiments for elucidating the mechanism and kinetics of the growth of graphene on liquid Cu, the confirmation of the dissolution of carbon in liquid Cu, and the TEM characterizations of the as-obtained graphene single crystal grown on liquid Cu.)



Shuting Zheng received her BSc from the Northwest University in 2016 and is now a master's degree candidate under the supervision of Prof. Lei Fu at the College of Chemistry and Molecular Sciences at Wuhan University. Her current research interest is the controllable growth of 2D material



Mengqi Zeng received her BSc from Wuhan University in 2013. She obtained her PhD degree under the supervision of Prof. Lei Fu in 2018 from Wuhan University. In 2018, she joined Wuhan University as an Associate Professor. Her current research interest is the catalyst design for the controllable growth and self-assembly of 2D materials.



Lei Fu received his BSc degree in chemistry from Wuhan University in 2001. He obtained his PhD degree from the Institute of Chemistry, Chinese Academy of Sciences in 2006. After obtaining his PhD, he worked as a Director's Postdoctoral Fellow at the Los Alamos National Laboratory, Los Alamos, NM (2006–2007). Thereafter, he became an Associate Professor at Peking University. In 2012, he joined Wuhan University as a Full Professor. His current interest of research focuses on the

controlled growth and novel property exploration of 2D atomic layer thin crystals.

化学气相沉积法在液态金属上快速生长石墨烯单晶

郑舒婷¹, 曾梦琪^{1*}, 曹慧¹, 张涛¹, 高晓雯¹, 肖遥², 付磊^{1,2*}

摘要 实现石墨烯大单晶的快速生长对于其未来在光电及电学器件领域的应用十分必要。目前已报道的在多晶金属衬底上生长石墨烯单晶的工作通常是通过降低前驱体供应量从而抑制成核来实现的,而这会显著降低成核以及后续生长的速度。新兴的液态金属催化剂具有准原子级平滑的表面和高扩散速率。理论上,液态金属是一个天然理想的基底,可同时实现低密度成核和快速生长。但截至目前,尚无工作探讨液态金属上石墨烯单晶的快速生长。在本研究中,我们成功地在液态铜表面实现了毫米级高质量石墨烯单晶的生长。液态铜中丰富的自由电子能加速石墨烯的成核,且其各向同性的平滑表面能显著抑制成核,使得成核密度较低。更重要的是,由于液态铜优异的可流动性,前驱体碳原子能实现快速扩散,这极大促进了石墨烯的生长,最高速率可达 $79 \mu\text{m s}^{-1}$ 。我们希望这一关于液态铜体系中石墨烯生长速率的研究能丰富研究者们对液态金属上二维材料生长行为的认知。我们也相信利用液态金属来实现石墨烯快速生长的策略能被拓展至其他二维材料,由此来促进它们在未来光电以及电学器件领域的应用。